Title

Absorption Function Loss Due to the History of Previous Ankle Sprain Explored by Unsupervised Machine Learning.

Xuemei Zhang[a], Issei Ogasawara[a,b], Shoji Konda[a,b], Tomoyuki Matsuo[a], Yuki Uno[a], Motoi Miyakawa[a], Izumi Nishizawa[a], Kazuki Arita[a], Jianting Liu[a], Ken Nakata[a]

Author affiliations

[a]Department of Health and Sport Sciences, Graduate School of Medicine, Osaka University, Osaka, Japan

[b]Department Sports Medical Biomechanics, Graduate School of Medicine, Osaka University, Osaka, Japan

Corresponding author

Issei Ogasawara, Ph.D.

Department of Health and Sport Sciences, Graduate School of Medicine, Osaka University

1-17, Machikaneyama-cho, Toyonaka city, Osaka, 560-0043, Japan

Tel: +81-6-6850-6032

Fax: +81-6-6850-6030

Email: ogasawara.issei.med@osaka-u.ac.jp

Acknowledgements

The authors are grateful to Dr. Shun Numasawa and Dr. Kumi Arimoto for providing the opportunities to collect data for this study. This study was supported by JSPS KAKENHI Grant Number 19K11491.

Manuscript details: Abstract = 291, Main text = 4510, Tables = 2, Figures = 4

Abstract

Background: Ankle sprains are common and cause persistent ankle function reduction. To biomechanically evaluate the ankle function after ankle sprains, the ground reaction force (GRF) measurement during the single-legged landing had been used. However, previous studies focused on discrete features of vertical GRF (vGRF), which largely ignored vGRF waveform features that could better identify the ankle function. **Purpose:** To identify how the history of ankle sprain affect the vGRF waveform during the single-legged landing with unsupervised machine learning considering the time-series information of vGRF. **Methods:** Eighty-seven currently healthy basketball athletes (12 athletes without ankle sprain, 49 athletes with bilateral, and 26 athletes with unilateral ankle sprain more than 6 months before the test day) performed single-legged landings from a 20 centimeters (cm) high box onto the force platform. Totally 518 trials vGRF data were collected from 87 athletes of 174 ankles, including 259 ankle sprain trials (from previous sprain ankles) and 259 non-ankle sprain trials (from without sprain ankles). The first 100 milliseconds (ms) vGRF waveforms after landing were extracted. Principal component analysis (PCA) was applied to the vGRF data, selecting 8 principal components (PCs) representing 96% of the information. Based on these 8 PCs, k-means method ($k = 3$) clustered the 518 trials into three clusters. Chi-square test assessed significant differences ($p < 0.01$) in the distribution of ankle sprain and non-ankle sprain trials among clusters. **Findings:** The ankle sprain trials accounted for a significantly larger percentage (63.9%) in Cluster 3, which exhibited rapidly increased impulse vGRF waveforms with larger peaks in a short time. **Significance:** PCA and k-means method for vGRF waveforms during single-legged landing identified that the history of previous ankle sprains caused a loss of ankle absorption ability lasting at least 6 months from an ankle sprain.

Keywords:

Vertical ground reaction force, History of ankle sprains, Principal component analysis, K-means, Clustering

1. Introduction

Ankle sprain is the most common type of acute sports trauma [1]. It often occurs in basketball, football, dance, and other sports, including violent landing or quick change of running direction movements [2] and disrupts the athlete's career [3]. For decades, many clinicians and biomechanics researchers have focused on preventing ankle sprain, however, recent epidemiology has shown that it continues to dominate the list of sports injuries [4]. A previous review showed that 53% of basketball injuries and 29% of football injuries were ankle sprains, and the average time loss of football players was 15 days [3]. Most people (45%–75%) who initially suffered from ankle sprain will experience deterioration which will lead to post-traumatic osteoarthritis of the ankle [5,6], joint instability [7,8], loss of shock absorption ability [8], and proprioception decrease [9] even after 6 months of ankle sprain [5]. Athletes who have suffered ankle sprains that can develop into chronic ankle instability, present reduced physical activity and recurrent giving way, which results in a decrease in the quality of life [5,10,11].

Single-legged landing combined with measuring the ground reaction force (GRF) is widely used to evaluate the ankle function of ankle-injured people [4,12,13]. The vertical component GRF (vGRF) observed in the single-legged landing is represented as a function of time in Figure S1 (See Supplemental material). The magnitude of vGRF begins to increase from the moment of the forefoot-floor contact and then an impact peak appears synchronous with the floor/heel impact. After that, vGRF gradually decreases to the amount of body mass. The most visually apparent characteristics of vGRF time signal might be the magnitude of impact peak (peak vGRF) and its appearance timing (peak time). Although previous studies have shown that participants with ankle instability had a larger peak vGRF and shorter time to peak vGRF than healthy participants during landing [13,14], a focus on discrete features alone may greatly ignore the other features that the temporal pattern of the vGRF waveforms contains. Therefore, it is meaningful to identify the vGRF waveform-oriented features related to the history of previous ankle sprains rather than discrete features.

Continuous waveform analysis is an alternative method of discrete feature analysis in unsupervised machine learning. It is becoming popular in many disciplines and reportedly provides better insight than discrete feature analysis [15]. The quantitative analysis of waveform is simplified by the dimension reduction to extract waveform features for downstream analysis. Principal component analysis (PCA) is one of the most common dimension reduction methods which consists of an orthogonal transformation that converts the variable into new uncorrelated principal components (PCs). In the clinical situation, PCA has been used to investigate the difference in the time-series kinetic and kinematic variables (waveform data) during walking between healthy people and osteoarthritis (OA) patients [16]. The clustering methods based on PC coefficients can be used to categorize different types of athletes according to the gait waveform [17]. The k-means method is also a popular clustering algorithm in unsupervised machine learning [18,19]. It has shown good results in clustering vGRF using the k-means method based on normalized data [20]. One of the merits of unsupervised clustering of vGRF data as compared to the pre-grouping (pre-labeling) comparison design (e.g., ankle sprained athletes vs. healthy athletes) is to avoid the risks of ignoring the degree of recovery from the ankle sprain. For example, to make it easier to distinguish the ankle function in most studies, previous studies filtered out the ankles that appear to have recovered but remain sprained through the inclusion criteria [21,22]. Although such a pre-grouping design may contrast the functional difference between healthy ankles and ankles with chronic instability, the potential functional loss in recovering ankles may not be elucidated (e.g., loss of ankle absorption function lasting more than six months since ankle sprain). Therefore, by clustering the GRF waveforms through unsupervised machine learning based on PCA-generated features, how the history of ankle sprain affects the ankle function can be examined without biased filtering of the participants or evaluator's arbitrary feature engineering.

The purpose of this study was to identify how the history of ankle sprain affected the vGRF waveform during single-legged landing. To this end, we introduced the PCA as a data-driven feature

engineering method combined with the k-means clustering method to evaluate the vGRF waveforms with and without the history of ankle sprain. We hypothesized that the PCA extracted the vGRF waveform features associated with loss of ankle absorption function, and the k-means-derived cluster of vGRF waveforms which includes higher percentage of ankle sprain trials demonstrated significantly greater vGRF peaks and earlier peak times than those of the other clusters. In the discussion, we considered what kind of functional alteration of the ankle happened due to the history of ankle sprain based on the clustering results.

2. Methods

2.1 Participants

Eighty-seven basketball athletes (54 males, 33 females, age: 16.3 ± 1.7 years, height: 1.7 ± 0.08 m, mass: 60.2 ± 10.1 kg) were recruited in this study. Athletes who had histories of severe lower limb injury that required surgical treatment (e.g., anterior cruciate ligament injury) or bone fracture in their athlete career were excluded from the candidate participants. In addition, athletes who had new lower limb injuries that required suspension of sports participation for more than 1 day within six months up to the experimental day were also excluded. The athletes who did not meet above excluding conditions with no subjective symptoms of ankle sprain (e.g., pain or swelling of joint and anxiety of athletic movement) in participating in sports practice or games were included. Therefore, the participants of this study included the athletes who met the following criteria: 1) those without previous lower limb injuries; 2) those with non-severe lower limb injuries that did not suspend basketball training or games within six months before the experimental day; and 3) those currently returned to sports with no subjective symptoms of ankle sprain. Demographic information of the participants was detailed in Table 1. A questionnaire was used to assess whether each participant had suffered from an ankle sprain. Participants who had the history of ankle sprain were requested to report the date of the ankle sprains. All participants provided informed consent before participating. This study was approved by the research ethics review board of Osaka University

Hospital (Approval No.19465).

2.2 Single-legged landing task

After a standardized dynamic warm-up (see Table S1, Supplemental material), the participants were asked to perform a single-legged landing task (Fig. 1). They were stood barefoot on a 20-centimeters (cm) high platform with the single leg behind a force plate (TFP404011B-A, Technology Service, Ltd. Nagano, JPN). Then they were instructed to jump off toward the center of force plate with the same leg. After landing, they were requested to hold the single-legged standing position for at least 5 seconds (s) while remaining static on the force plate. The order of the side of the jump-landing leg (left or right) was randomly determined and six trials for each leg were performed (a total of 12 trials per participant). The interval time between trials was 5 s. The switch between jump-landing legs was accompanied by a one-minute rest period. The participants were asked to keep their arms crossed in front of their chest to avoid the arm-dominant balancing strategy during landing. When the participant landed with both feet, the contralateral leg touched the force plate or failed to keep 5 s static standing, the trial was regarded as a fail and discarded from the analysis. If failed trials occurred, additional trials were not performed to avoid the potential effects of fatigue and postural adaptation. The GRF data was recorded at a 1 kHz sampling frequency. None of the participants in this study reported subjective difficulties with the landing technique, ankle joint pain, or lower limb discomfort during the experiment.

2.3 Data analysis

The custom scripts written in Python 3.10 on the PyCharm Professional IDE (Version 2022.2.4, JetBrains, Czech) were used for data analysis. A total of 895 trials of 87 athletes (174 legs) were included in this study, while 149 failed trials were ruled out. The maximum number of failed trials out of 6 total trials was 2. None of the athletes failed more than 3 trials. The vGRF data were filtered using a 2^{nd} order Butterworth digital filter (zero-lag, low-pass, cutoff frequency: 100 Hz) to remove

the force plate specific high-frequency noise and then extracted 101 samples of time-series data from 0 to 100 milliseconds (ms) after initial contact (IC) that was defined as vGRF larger than 10 Newtons (N). All vGRF data were normalized by the participant's body mass (N). The unit of the normalized vGRF was therefore unitless. The set of trials performed by those participants with previous ankle sprains were labeled as the ankle sprain trial group (n = 636), and the set of trials performed by those participants without ankle sprains were labeled as the non-ankle sprain trial group (n = 259) based on the reported history of ankle sprain. To equalize the number of trials between trial groups, 259 trials were randomly selected from 636 trials as the ankle sprain trial group. Random selection of the trials was performed with "random.sample" function (version: 3.10.13, https://docs.python.org/3.10/library/random.html) in Python. For the PCA, we first created a data matrix $\boldsymbol{X}$ (518 × 101, e.g., size of 259 trials from two trial groups × 101 time points). After column-wise standardization of the data matrix $\boldsymbol{X}$, the eigen-decomposition of the covariance matrix of $\boldsymbol{X}$ was performed to obtain 101 eigenvalues (Principal Components; PCs) and corresponding 101 eigenvectors. The parallel analysis was used to determine the number of PCs for the subsequent k-means clustering [23], and the first 8 major PCs were retained (See Figure S2 in Supplemental material).

For the clustering of 8 PCs using k-means method, this study attempted to determine the number of k using the elbow method [24]. The result of elbow method recommended the number of k = 3 was the best (see Figure S3 in Supplemental material). In clinical interpretation, considering that the current participants with ankle sprains were at least six months removed from their most recent injury, it was anticipated that there might be three groups based on the recovery status of the ankle, e.g., fully recovered as healthy ankle, in the process of recovering, and insufficient recovery from the ankle sprain. The k-means algorithm with the "k-means++" method and a maximum of 500 iterations, which belongs to the *Clustering* module in *scikit-learn* (version 1.2.2, https://scikit-learn.org/stable/modules/clustering.html), divided the first 8 major PCs into three clusters.

2.4 Statistical Analysis

To determine the vGRF waveform distribution of each cluster in the ankle sprain trial group and the non-ankle sprain trial group, the number of trials in each cluster was recorded in a contingency table. Pearson's independent Chi-square test was used to determine whether the cluster distribution occurred by chance or whether there was a statistically significant difference between the observed distribution and the expected distribution which represents the relationship between the cluster and the history of ankle sprain. Bonferroni correction was used to determine whether there was a statistically significant difference between the ankle sprain trial group and the non-ankle sprain trial group in each cluster ($p < 0.017$). To quantitatively evaluate the difference of vGRF waveforms in three clusters, the peak vGRF and peak time were compared between clusters with Welch's analysis of variance (ANOVA) and then Game Howell post-hoc analysis detected the differences between every two clusters ($p<0.017$). The statistical procedures used the SciPy (version 1.10.0, https://scipy.org/), Statsmodels (version 0.13.0, https://pingouin-stats.org/build/html/index.html), and Pingouin modules (version 0.5.3, https://pingouin-stats.org/build/html/index.html) in Python 3.10.

3.Results

3.1 Result of PCA

The first 8 major PCs selected according to the parallel analysis explained the 96% variance of the raw vGRF waveform dataset (See Figure S4 in Supplemental material).

3.2 Clusters of vGRF based on the first 8 major PCs

The k-means clustering method ($k = 3$) divided the first 8 major PCs (a total of 518 trials) into three distinct clusters (Fig. 2). The largest cluster was Cluster 1 which included 259 trials. The second largest cluster was Cluster 2, including 187 trials. The smallest cluster was Cluster 3, which had 72

213 trials. The normalized vGRF waveforms allocated for each cluster and the ensemble-averaged
214 waveform for each cluster were shown in Figure 3. Welch's ANOVA and post-hoc analysis revealed
215 that there were significant differences in vGRF peak value and peak time among the clusters (Fig.
216 4). Cluster 1 had the smallest vGRF peak of 3.72 [standard deviation (SD): 0.58] and a significantly
217 slower peak time of 61.9 [SD: 6.4] ms than the other Clusters (Fig. 4).
218
219 For the details, the magnitude of vGRF in Cluster 1 constantly increased from 0 to 50 ms after IC,
220 reaching twice the body mass around 50 ms. After reaching an inflection point there, it peaked
221 around 60 ms (Fig. 3a). Cluster 2 took about 40 ms to increase to twice the body mass and produced
222 a peak of 4.0 [SD: 0.6] around 50 ms, which was significantly larger than Cluster 1 (Fig.3b). Cluster
223 3 had a steeper rise slope than the other clusters, taking only about 30 ms to reach twice the body
224 mass and producing a peak of 4.5 [SD: 0.7], which was significantly greater than the other clusters
225 at about 40 ms (Fig.3c). Overlaying the vGRF waveforms for each cluster, the difference in the
226 timing of waveform rise toward the peak was visually apparent (Fig.3d). The loading vectors of the
227 8 PCs derived from PCA were displayed in Fig. 3e. The absolute value of the loading vector of a
228 certain PC is an indicator of how much that PC contributed to the variation of the set of waveforms.
229 The absolute values of the loading vectors were less than 0.1 from 0 to 20 ms after IC where the
230 vGRF of all clusters showed similar magnitudes (Fig.3d and 3e), assuming that the absolute value
231 of loading vectors less than 0.1 represented the small variation in our dataset. The loading vectors
232 of PC1, 2, and 4 began to increase more than 0.1 around 30 ms after IC. It was temporarily
233 corresponded with the timing of that the vGRF of Cluster 3 began to separate from the other clusters
234 in the force development phase. Even after the vGRF of Cluster 1 reached its peak around 60 ms,
235 the absolute value of the loading vectors of PC1, 2, and 3 still showed absolute values of more than
236 0.1, reflecting the variation of vGRF waveforms among clusters even after impact peaks. PCA
237 retuned the major PCs (from 1 to 4) reflecting the non-discrete waveform variation appeared from
238 20 ms to 60 ms after IC.
239

3.3 Relationship between the history of ankle sprain and clusters

There was a statistically significant relationship between the history of ankle sprain and the clusters (Pearson Chi-square test $p < 0.01$, Table 2). The percentage of ankle sprain and non-ankle sprain trial groups in the clusters weas calculated (Table 2). Bonferroni correction showed that there was a significant difference in the percentage between the ankle sprain and non-ankle sprain trial group in the smallest Cluster 3 (63.8% vs 36.1%, $p = 0.0054$), but not in Cluster 1 (51.4% vs 48.6%, $p = 0.78$) and 2 (42.8% vs 57.2%, $p = 0.15$).

4. Discussion

This study aimed to determine how the history of ankle sprain affected the vGRF waveform using PCA feature engineering method and k-means clustering method. To the best of our knowledge, this is the first study to cluster vGRF data for investigating the ankle function with the history of ankle sprains using unsupervised machine learning methods. The ankle sprain trials significantly more concentrated in the smallest Cluster 3 (ankle sprain trial group vs non-ankle sprain trial group: 63.8% vs 36.1%, $p=0.0054$). The vGRF waveforms involved into Cluster 3 was characterized by a rapid increase and early peaking of vGRF (Fig 3). This characteristics of vGRF waveform was similar to those of unstable ankles reported in the previous literatures [13,14]. It is suggested that the shock-absorbing function of the ankle joint had deteriorated, even though at least 6 months had passed since the last ankle sprain. The results of this study supported our hypothesis that the vGRF waveforms were affected by previous ankle sprains because the clustering of vGRF waveforms indicated the difference in the ankle absorption function among the trial groups.

4.1 The PCA extracted the important vGRF features.

We selected 8 major PCs (8-dimension features) out of 101-dimension vGRF data from PCA to capture the inter-trial variability of vGRF dataset according to the parallel analysis. In previous studies, typically few numbers of discrete features, such as the peak vGRF [12,13,25,26], peak

vGRF time [2,12,13,26], and the rate of force development [27], have been arbitrarily selected to evaluate the characteristics of landing movements. Although these discrete features seem easy to be selected by the evaluator, it is clear that a small number of discrete features (e.g., peak and peak time) are less capable of representing the variety of vGRF waveform profile during single-legged landing than the 8 PCs extracted by PCA. The magnitudes of loading vectors of 8 PCs began to increase around 30 ms (Fig. 3e), which coincided with the timing of the steep rise of the vGRF waveform in Cluster 3 in particular. This feature did not exist in Cluster 1 and 2. In addition, the loading vectors of PC 1 to PC 3 still had larger absolute value of more than 0.1 around 60 to 80 ms even after the time of peak vGRF. This indicated that the PCA retained meaningful information involved in the vGRF waveforms even after its peak time. The discrete features, such as peak vGRF or its appearance time cannot solely express such waveform-oriented characteristics. Therefore, PCA was considered essential as a pre-processing step for meaningful clustering.

4.2 The difference showed in Cluster 3 between the ankle sprain and non-ankle sprain trial groups.

High rate of ankle sprain trials in Cluster 3 suggested that the history of ankle sprains may result in a loss of ankle absorption ability which lasts at least six months after injury during landing motion. This statement was supported by the vGRF waveforms of Cluster 3, characterized by a significantly larger vGRF peaks appearing in a short time than those of the other Clusters (Fig. 4). Although all the participants who had histories of ankle sprains were satisfied with the inclusion criteria (e.g., at least six months have passed from the latest light to moderate lower limb trauma and currently no subjective symptoms of ankle sprain in participating in sports), the calf musculature and foot's intrinsic muscles perhaps did not properly perform those eccentric contractions and resulting in a high energy heel impact during landings [11,28]. Although other previous studies have found a reduction in shock absorption function after ankle sprains, it is interesting to note that this study used a different approach than previous studies, which was using clustering with unsupervised machine learning to obtain consistent results. The conventional approach in previous studies was

first to separate the participants into two groups, i.e., ankle sprained group and healthy control group, and then the features, which were arbitrary selected so as to reflect the ankle absorption function (e.g., peak vGRF or peak time), were compared between the groups [2,13,29]. Such a comparative design and feature selection may constrain the research focus on the ankle absorption function. In contrast, the data-driven exploratory approach adopted in this study automatically clustered all the vGRF waveforms into the sub-groups without label of history of ankle sprains. As a result, we have confirmed that the Cluster 3 (involving a higher rate of ankle strain trials) demonstrated the high energy vGRF waveforms during single-legged landing (Fig. 3c). This result suggested that the decreased shock absorption capacity lasting at least six months influenced the vGRF waveforms during landing and the difference of recovery level in shock absorption capacity among participants produced the variation of vGRF waveform. Using PCA characterized the variations in the set of vGRF waveforms as 8 PCs, the k-means method separated the trials so as to reflect the reduced shock absorption capacity in Cluster 3 as distinct from the other clusters. Therefore, our approach and findings further consolidated the findings of the previous studies that a history of an ankle sprain results in a loss of shock absorption ability lasting at least six months [7,8].

4.3 Trials in Clusters 1 and 2 reflected recovery state of ankles with previous sprain.

The ankle sprain trial group clustered in Clusters 1 and 3 might reflect the different recovery status of ankles with previous sprain. The ankle sprain trials in Cluster 1 reflected more recovered shock-absorbing function of ankle than the trials in Cluster 3. This is supported by the significantly lower peak value and significantly slower peak time of vGRF waveform in Cluster 1 compared to Cluster 3 (Fig. 4). In addition, Cluster 1 included the vGRF waveforms showing a particularly slower time to peak (from 60 to 80 ms) reflective of successful elongation of shock-absorbing duration and reduction of peak vGRF (Fig 3a). Given that all the athletes had participated in sports activities with no subjective symptoms of ankle sprain on the test day, Cluster 1 included over half of trials (259 of 518 trials) with no significant difference in the percentage of ankle sprain trials and non-ankle sprain trails (51.4% vs. 48.6%, $p = 0.78$). Therefore, the trials with histories of ankle sprains in

Cluster 1 may considered to have regained the shock absorption function, similar to that of healthy individuals. Cluster 2 had the second largest number of trials after Cluster 1, and although there was no significant difference in the percentage of ankle sprain trials and non-ankle sprain trials (42.8% vs. 57.2%, p=0.15), the peak vGRF values and peak times were intermediate between the Clusters 1 and 3. This suggested that the ankle sprain trials clustered in Cluster 2 reflected the state of ankles in the process of recovering their shock-absorbing function. These characteristics suggest that our PCA and k-means methods can serve as a classifier to represent the degree of recovery from an ankle sprain.

5. Future perspective and clinical implication

As a clinical application, the current model (k-means with PCs) might work as a clinical test to determine the degree of recovery of shock absorption function of sprained ankles. Such application of the learned model primarily covers the return to play of basketball players with a history of ankle sprain. In addition, it is also noted that 26/72 (36.1%) trials of Cluster 3 were from ankles without previous ankle sprains. This result suggested that the current model may serve as a predictor of future ankle sprains. We will prospectively examine whether ankles that are currently healthy but exhibit high impact vGRF will suffer future ankle sprains or not. So, we need to apply the current model to a new dataset of different athletes to confirm the robustness of the model and prospectively follow up on the occurrence of ankle sprains. In the process, we will also work to improve the performance of the model itself. The future study should examine whether other feature engineering methods (e.g., functional principal component analysis) or unsupervised machine learning (e.g., hierarchical clustering) can better detect ankle joint dysfunction than the combined PCA and k-means model used in this study. This study identified the ankle joints having impaired shock absorption function in Cluster 3 by focusing on vGRF waveform profiles rather than discrete features of vGRF. This indicated that feature selection focusing on waveform profiles with time signals, rather than discrete features, contributes to evaluating ankle joint function with higher resolution. Therefore, it is necessary to further investigate which of the feature engineering methods

that utilizes the temporal change of signal [30] can improve the performance of evaluating the ankle joint function with the history of ankle sprains.

6. Limitation

This study only analyzed the vertical GRF and obtained the results associated with the ankle absorption function. However, this conclusion does not necessarily mean that the type of ankle function loss due to previous ankle sprains is limited to the loss of the absorption function. The frontal plane GRF component may reflect the ankle's mediolateral instability due to the damage of anterior talofibular ligament. The sagittal plane GRF component may be affected by the limited range of motion of ankle joints due to the history of ankle sprain [2,29]. The different kind of ankle dysfunction perhaps appears if the data of interest is different. Future studies which focus on the different GRF component (i.e., anterior/posterior and medial/lateral components) may provide comprehensive understanding of the ankle dysfunction due to the history of ankle sprain. The targeted athletes covered by this study were young Japanese basketball players. Since it was difficult to rule out the possibility that the model overfits the vGRF characteristics of our specific participants, caution is required in generalizing the results of this study to basketball players of another age group, other sports, or players from other regions. The age range of our participants was very limited (Age:16.3 ± 1.7 years). While this contributes to eliminating the effects of age differences in clustering results, it also inhibits generalization to basketball players in higher age groups (e.g., 20-30-year-olds). It is challenging to conclude only for this study, and it will be a subject for future work. However, the age group that this study targeted showed the highest incidence of ankle sprains (7.2 per 1,000 person-years for those 15 to 19 years of age [31]), and in Japan, a large-scale survey revealed that 9.4 % of young athletes in both genders have experienced ankle sprain injury in their careers [32], making it a severe problem. Therefore, it is significant to study the data set of adolescents first.

7. Conclusion

The 87 basketball athletes' vGRF waveforms with different absorption functions were evaluated by PCA and k-means clustering methods, and whether the history of previous ankle sprains was related to clustering was further discussed in this study. The vGRF waveforms were clustered into three different clusters that were confirmed to have a significant relationship with the history of ankle sprain through the Chi-square test ($p<0.01$). Bonferroni correction showed that there was a significant difference in the percentage between the ankle sprain and non-ankle sprain trial group in the smallest Cluster 3 (63.8% vs 36.1%, $p=0.0054$), but not in Cluster 1 (51.4% vs 48.6%, $p=0.78$) and 2 (42.8% vs 57.2%, $p=0.15$). The vGRF waveform rose slowly in Cluster 1, which is characterized by a smaller peak vGRF and a longer time to peak vGRF. In Cluster 3, the vGRF waveform rose rapidly, with a larger peak vGRF and a shorter time to peak vGRF. The vGRF waveform trend and peak characteristics in Cluster 2 were between Cluster 1 and Cluster 3. This study found that the vGRF with the history of ankle sprain had a similar percentage in Cluster 1 and a larger percentage in Cluster 3 than that without the history of ankle sprain, indicating that the vGRF impact phase may be affected by the previous ankle sprains.

Conflict of interest

None.

Author contributions

X.Z., I.O., S.K., T.M., and K.N. conceptualized and designed the study.

I.O. organized the experiments.

I.O., Y.U., M.M., I.N., K.A., and J.L. performed the experiments and data collection.

X.Z. and I.O. analyzed the data and performed the statistical analysis.

X.Z. and I.O. wrote the manuscript.

I.O., Y.U., S.K, T.M., M.M., I.N., K.A., J.L., and K.N. reviewed the manuscript, suggested corrections, and approved its final version.

400

401

402

403

404

405

406

Reference

[1] D.T.-P. Fong, Y. Hong, L.-K. Chan, P.S.-H. Yung, K.-M. Chan, A Systematic Review on Ankle Injury and Ankle Sprain in Sports, Sports Med. 37 (2007) 73–94. https://doi.org/10.2165/00007256-200737010-00006.

[2] E. Delahunt, K. Monaghan, B. Caulfield, Changes in lower limb kinematics, kinetics, and muscle activity in subjects with functional instability of the ankle joint during a single leg drop jump, J. Orthop. Res. 24 (2006) 1991–2000. https://doi.org/10.1002/jor.20235.

[3] Z. Flore, K. Hambly, K.D. Coninck, G. Welsch, Time-loss and recurrence of lateral ligament ankle sprains in male elite football: A systematic review and meta-analysis, Scand. J. Med. Sci. Sports. 32 (2022) 1690–1709. https://doi.org/10.1111/sms.14217.

[4] C. Doherty, C. Bleakley, J. Hertel, B. Caulfield, J. Ryan, E. Delahunt, Ankle sprain and landing performance, Scand. J. Med. Sci. Sports. 25 (2015) 806–817. https://doi.org/10.1111/sms.12390.

[5] P.A. Gribble, C.M. Bleakley, B.M. Caulfield, C.L. Docherty, F. Fourchet, D.T.-P. Fong, J. Hertel, C.E. Hiller, T.W. Kaminski, P.O. McKeon, K.M. Refshauge, E.A. Verhagen, B.T. Vicenzino, E.A. Wikstrom, E. Delahunt, 2016 consensus statement of the International Ankle Consortium: prevalence, impact and long-term consequences of lateral ankle sprains, Br. J. Sports Med. 50 (2016) 1493. https://doi.org/10.1136/bjsports-2016-096188.

[6] A. Theisen, J. Day, Chronic Ankle Instability Leads to Lower Extremity Kinematic Changes During Landing Tasks: A Systematic Review., Int. J. Exerc. Sci. 12 (2019) 24–33. https://www.ncbi.nlm.nih.gov/pmc/articles/PMC6355117/.

[7] J.P. Gerber, G.N. Williams, C.R. Scoville, R.A. Arciero, D.C. Taylor, Persistent Disability Associated with Ankle Sprains: A Prospective Examination of an Athletic Population, Foot Ankle Int. 19 (1998) 653–660. https://doi.org/10.1177/107110079801901002.

[8] R.J. Brison, A.G. Day, L. Pelland, W. Pickett, A.P. Johnson, A. Aiken, D.R. Pichora, B. Brouwer, Effect of early supervised physiotherapy on recovery from acute ankle sprain: randomised controlled trial, BMJ. 355 (2016) i5650. https://doi.org/10.1136/bmj.i5650.

[9] A.S.N. Fu, C.W.Y. Hui-Chan, Ankle Joint Proprioception and Postural Control in Basketball Players with Bilateral Ankle Sprains, Am. J. Sports Med. 33 (2005) 1174–1182. https://doi.org/10.1177/0363546504271976.

[10] P.A. Gribble, R.E. Kleis, J.E. Simon, L.I. Vela, A.C. Thomas, Differences in health-related quality of life among patients after ankle injury, Front. Sports Act. Living. 4 (2022) 909921. https://doi.org/10.3389/fspor.2022.909921.

[11] A. Anandacoomarasamy, L. Barnsley, L. Grujic, Long term outcomes of inversion ankle injuries, Br. J. Sports Med. 39 (2005) e14. https://doi.org/10.1136/bjsm.2004.011676.

[12] C. Brown, D. Padua, S.W. Marshall, K. Guskiewicz, Individuals with mechanical ankle instability exhibit different motion patterns than those with functional ankle instability and ankle sprain copers, Clin. Biomech. 23 (2008) 822–831. https://doi.org/10.1016/j.clinbiomech.2008.02.013.

[13] R.D. Ridder, T. Willems, J. Vanrenterghem, M.A. Robinson, T. Palmans, P. Roosen, Multi-segment foot landing kinematics in subjects with chronic ankle instability, Clin. Biomech. 30 (2015) 585–592. https://doi.org/10.1016/j.clinbiomech.2015.04.001.

[14] H.G. Jeon, S.Y. Lee, S.E. Park, S. Ha, Ankle Instability Patients Exhibit Altered Muscle Activation of Lower Extremity and Ground Reaction Force during Landing: A Systematic Review and Meta-Analysis, J. Sports Sci. Med. 20 (2021) 373–390. https://doi.org/10.52082/jssm.2021.373.

[15] C. Richter, N.E. O'Connor, B. Marshall, K. Moran, Analysis of Characterizing Phases on Waveforms: An Application to Vertical Jumps, J. Appl. Biomech. 30 (2014) 316–321. https://doi.org/10.1123/jab.2012-0218.

[16] K.J. Deluzio, J.L. Astephen, Biomechanical features of gait waveform data associated with knee osteoarthritis An application of principal component analysis, Gait Posture. 25 (2007) 86–93. https://doi.org/10.1016/j.gaitpost.2006.01.007.

[17] T.M. Guess, A.D. Gray, B.W. Willis, M.M. Guess, S.L. Sherman, D.W. Chapman, J.B. Mann, Force-Time Waveform Shape Reveals Countermovement Jump Strategies of Collegiate Athletes, Sports. 8 (2020) 159. https://doi.org/10.3390/sports8120159.

[18] S. Lloyd, Least squares quantization in PCM, IEEE Transactions on Information Theory. 28 (1982) 129–137. https://doi.org/10.1109/tit.1982.1056489.

[19] P.J. Jones, M. Catt, M.J. Davies, C.L. Edwardson, E.M. Mirkes, K. Khunti, T. Yates, A.V. Rowlands, Feature selection for unsupervised machine learning of accelerometer data physical activity clusters – A systematic review, Gait Posture. 90 (2021) 120–128. https://doi.org/10.1016/j.gaitpost.2021.08.007.

[20] C. Richter, N.E. O'Connor, B. Marshall, K. Moran, Clustering vertical ground reaction force curves produced during countermovement jumps, J Biomech. 47 (2014) 2385–2390. https://doi.org/10.1016/j.jbiomech.2014.04.032.

[21] H. Tajdini, Z. Mantashloo, A.C. Thomas, A. Letafatkar, G. Rossettini, Inter-limb asymmetry of kinetic and electromyographic during walking in patients with chronic ankle instability, Sci Rep-Uk. 12 (2022) 3928. https://doi.org/10.1038/s41598-022-07975-x.

[22] T. Watabe, T. Takabayashi, Y. Tokunaga, T. Watanabe, M. Kubo, Copers exhibit altered ankle and trunk kinematics compared to the individuals with chronic ankle instability during single-leg landing, Sport Biomech. (2022) 1–13. https://doi.org/10.1080/14763141.2022.2058989.

[23] J.C. Hayton, D.G. Allen, V. Scarpello, Factor Retention Decisions in Exploratory Factor Analysis: a Tutorial on Parallel Analysis, Organ. Res. Methods. 7 (2004) 191–205. https://doi.org/10.1177/1094428104263675.

[24] D.M. SAPUTRA, D. SAPUTRA, L.D. OSWARI, Effect of Distance Metrics in Determining K-Value in K-Means Clustering Using Elbow and Silhouette Method, Proc. Sriwij. Int. Conf. Inf. Technol. Appl. (SICONIAN 2019). (2020) 341–346. https://doi.org/10.2991/aisr.k.200424.051.

[25] M. Lee, C. Youm, M. Son, J. Kim, Y. Kim, Effects of chronic ankle instability and induced mediolateral muscular fatigue of the ankle on competitive taekwondo athletes, J. Phys. Ther. Sci. 29 (2017) 1329–1335. https://doi.org/10.1589/jpts.29.1329.

[26] X. Zhang, J. Aeles, B. Vanwanseele, Comparison of foot muscle morphology and foot kinematics between recreational runners with normal feet and with asymptomatic over-pronated feet, Gait Posture. 54 (2017) 290–294. https://doi.org/10.1016/j.gaitpost.2017.03.030.

[27] K.B. Kosik, M.C. Hoch, J.T. Hartzell, K.A. Bain, S. Slone, P.A. Gribble, Jump landing among chronic ankle instability individuals who did or did not attend rehabilitation at the time of injury, Phys. Ther. Sport. 57 (2022) 26–32. https://doi.org/10.1016/j.ptsp.2022.07.005.

[28] M.J. Decker, M.R. Torry, D.J. Wyland, W.I. Sterett, J.R. Steadman, Gender differences in lower extremity kinematics, kinetics and energy absorption during landing, Clin. Biomech. 18 (2003) 662–669. https://doi.org/10.1016/s0268-0033(03)00090-1.

[29] B. Caulfield, M. Garrett, Changes in ground reaction force during jump landing in subjects with functional instability of the ankle joint, Clin. Biomech. 19 (2004) 617–621. https://doi.org/10.1016/j.clinbiomech.2004.03.001.

[30] D. Boe, A.A. Portnova-Fahreeva, A. Sharma, V. Rai, A. Sie, P. Preechayasomboon, E. Rombokas, Dimensionality Reduction of Human Gait for Prosthetic Control, Front. Bioeng. Biotechnol. 9 (2021) 724626. https://doi.org/10.3389/fbioe.2021.724626.

[31] B.R. Waterman, B.D. Owens, S. Davey, M.A. Zacchilli, P.J. Belmont, The Epidemiology of Ankle Sprains in the United States, J. Bone Jt. Surg. 92 (2010) 2279–2284. https://doi.org/10.2106/jbjs.i.01537.

[32] J. Iwamoto, T. Takeda, Y. Sato, H. Matsumoto, Retrospective case evaluation of gender differences in sports injuries in a Japanese sports medicine clinic, Gend. Med. 5 (2008) 405–414. https://doi.org/10.1016/j.genm.2008.10.002.

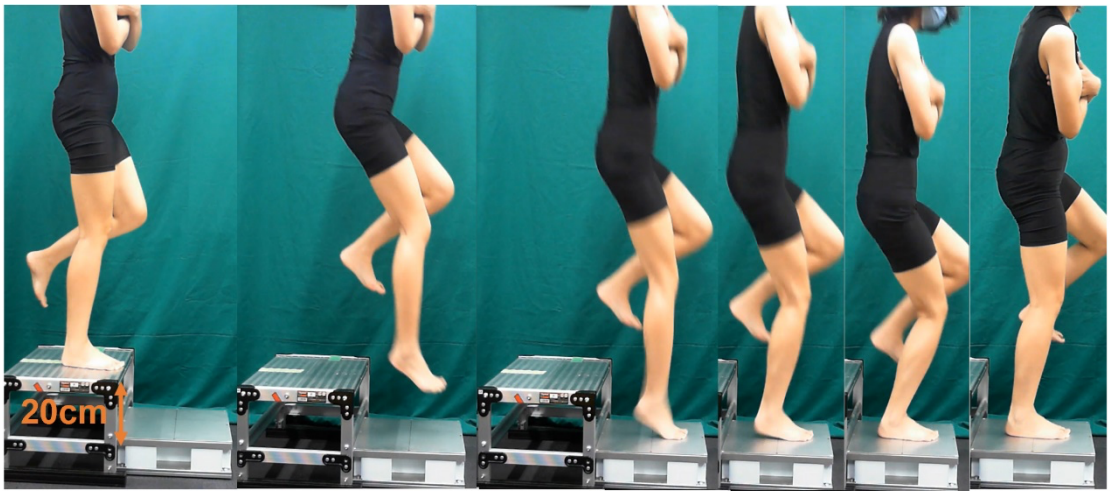

Figure 1. Single-legged landing task

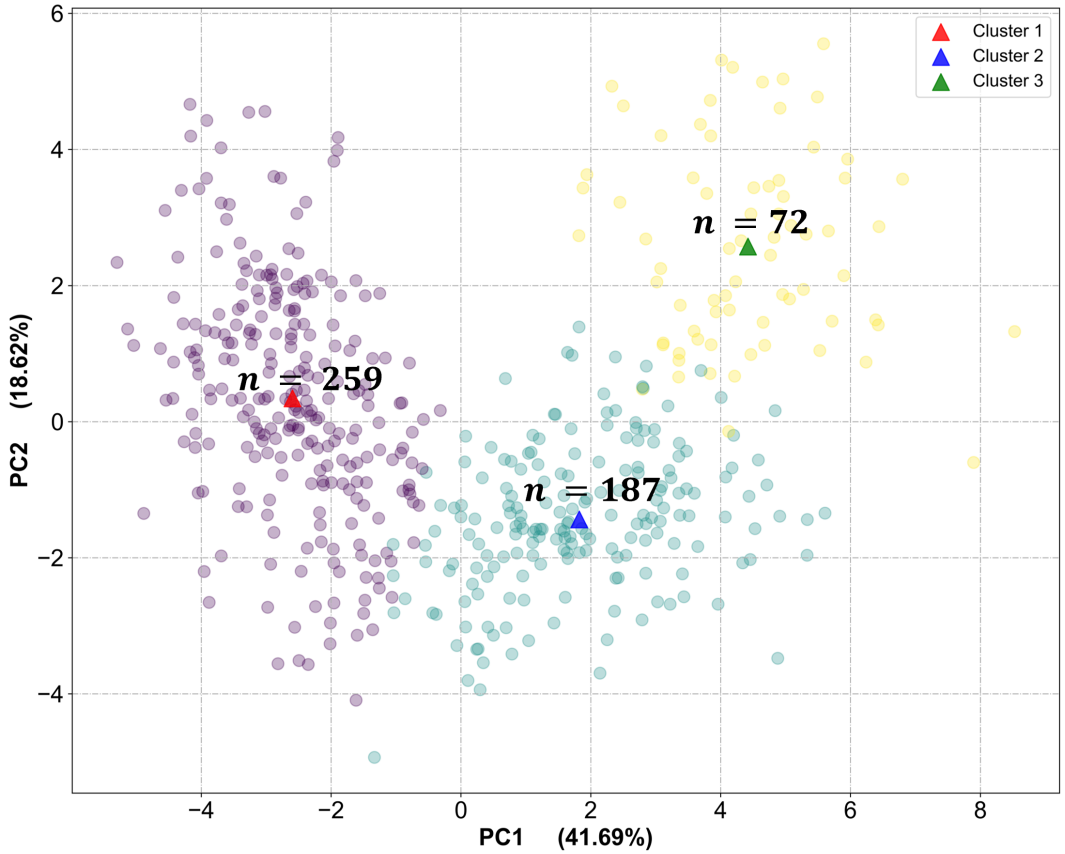

Figure 2. Scatterplot of the first two PCs (PC1 and PC2 of vGRF waveform) classified by k-means method (k = 3). The purple dots indicated Cluster 1, green dots indicated Cluster 2, gold dots indicated Cluster 3. The triangle means the center of each cluster. The number above the center of the cluster represents the number of trials that the cluster includes.

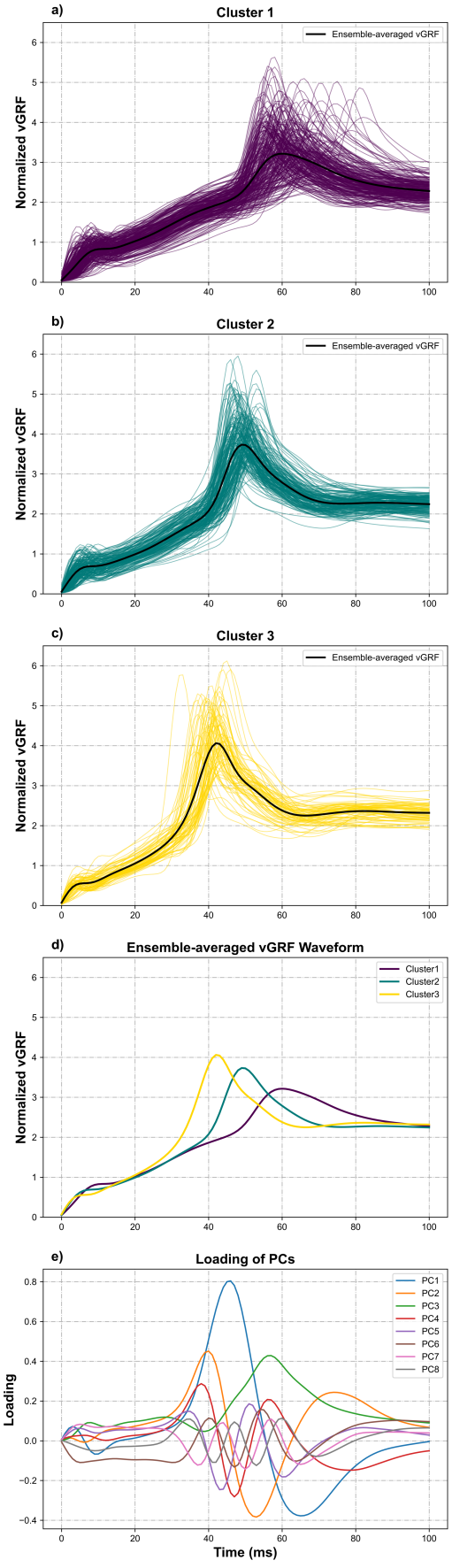
a)
Cluster 1
Ensemble-averaged vGRF
Normalized vGRF
b)
Cluster 2
Ensemble-averaged vGRF
Normalized vGRF
c)
Cluster 3
Ensemble-averaged vGRF
Normalized vGRF
d)
Ensemble-averaged vGRF Waveform
Cluster1
Cluster2
Cluster3
Normalized vGRF
e)
Loading of PCs
PC1
PC2
PC3
PC4
PC5
PC6
PC7
PC8
Loading
Time (ms)

Figure 3. Normalized vGRF waveforms classified into three clusters and loading vectors of 8 PCs.

a) Cluster 1, b) Cluster 2, and c) Cluster 3. The black solid line indicated ensemble-averaged vGRF waveform. d) Showed the ensemble-averaged vGRF waveform of each cluster in one panel. e) Showed the loading vectors of eight PCs.

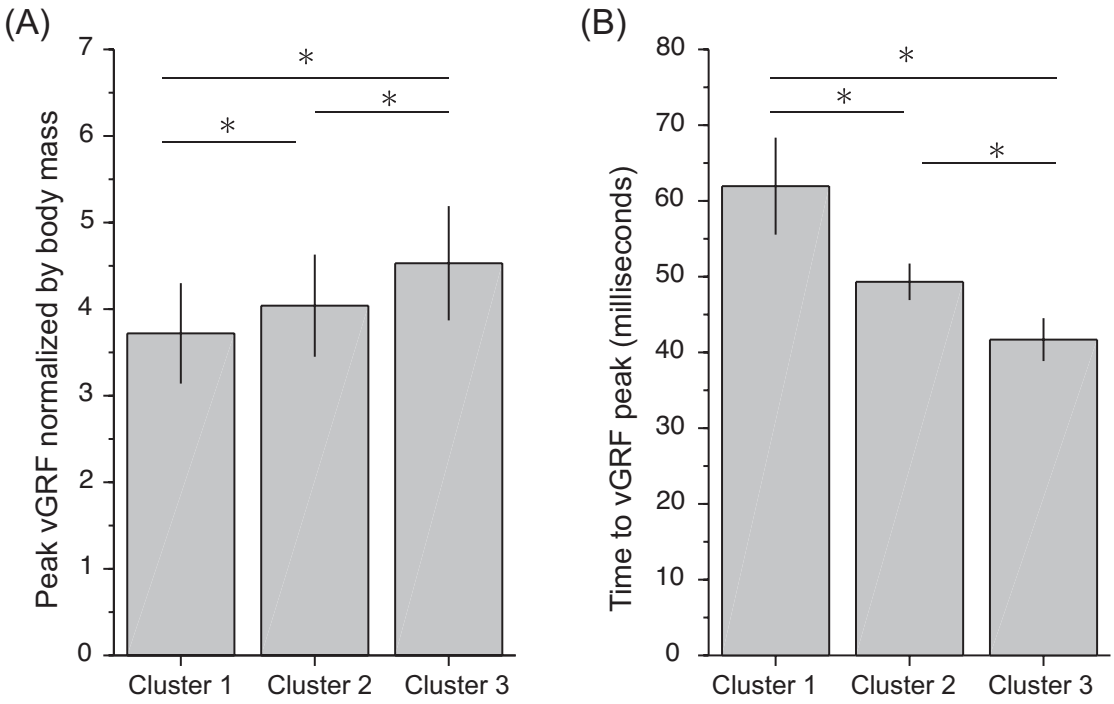

Figure 4. Inter cluster comparison of averaged peak vertical ground reaction force (vGRF) and the averaged time to vGRF peak. The asterisk denoted that there was a significant difference ($p<0.017$, Welch's analysis of variance and Game Howell post-hoc analysis. P value was corrected with Bonferroni correction).

Table 1. Demographic information of participants

Demographic characteristics	All	Without ankle sprain	With ankle sprains	
			Unilateral	Bilateral
	(n = 87)	(n = 12)	(n = 26)	(n = 49)
Age (years), mean (SD)	16.4 (1.8)	14.8 (1.9)	17.4 (1.5)	16.3 (1.7)
Gender (male), n (%)	56 (60.7)	4 (33.3)	14 (53.8)	54 (73.5)
Weight (kilograms), mean (SD)	59.3 (10.5)	48.6 (11.0)	62.5 (8.0)	60.2 (10.1)
Height (meters), mean (SD)	1.7 (0.10)	1.6 (0.09)	1.7 (0.10)	1.7 (0.08)
Body mass index, mean (SD)	20.9 (2.5)	18.8 (2.9)	21.5 (1.5)	21.0 (2.7)
Experience of basketball (years), mean (SD)	6.2 (2.8)	4.9 (3.0)	7.6 (2.5)	5.7 (2.7)
Days since last ankle sprain (days), mean (SD)	354.8 (292.5)	NAN	442.4 (210.8)	395.2 (304.7)

Note: Very light ankle sprains which did not require suspension of sports participation were included.

Table 2. Contingency table of the number and percentage of vGRF trials in each cluster.

Group \ Clusters	Number of trials			
	Cluster 1	Cluster 2	Cluster 3*	Total
Ankle Sprain trials	133 [51.4%]	80 [42.8%]	46 [63.8%]	259
Non-ankle Sprain trials	126 [48.6%]	107 [57.2%]	26 [36.1%]	259
Total	259	187	72	518
P-value for Bonferroni Correction	p = 0.780	p = 0.150	p = 0.005	

Chi-square test p = 0.0081

* Significant difference between ankle sprain and non-ankle sprain trial groups.

Supplemental Material

Absorption Function Loss Due to the Histories of Ankle Sprain Explored by Unsupervised Machine Learning.

Xuemei Zhang[a], Issei Ogasawara[a,b], Shoji Konda[a,b], Tomoyuki Matsuo[a], Yuki Uno[a], Motoi Miyakawa[a], Izumi Nishizawa[a], Kazuki Arita[a], Jianting Liu[a], Ken Nakata[a]

[a]Department of Health and Sport Sciences, Graduate School of Medicine, Osaka University, Osaka, Japan

[b]Department Sports Medical Biomechanics, Graduate School of Medicine, Osaka University, Osaka, Japan

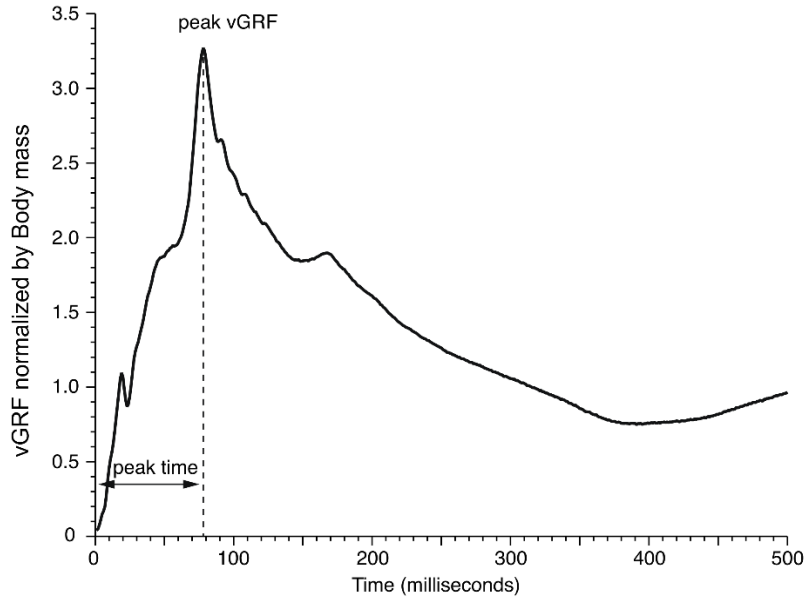

Figure S1. Representative vertical ground reaction force waveform during single-legged landing.

Time zero means the timing of initial forefoot-floor contact (IC). vGRF: vertical ground reaction force.

Table S1. A standardized warm-up exercises.

Exercise	**Duration**	**Explanation**
Walking and jogging	3 minutes	Free walking and jogging on the basketball court.
Range of motion exercise of ankle joint	1 minutes	Rotating the ipsilateral ankle joint with the standing position. Thirty seconds for each ankle joint.
Stretching of calf	1 minutes	Static stretching of the calf musculatures with standing position. Thirty seconds for each side.
Stretching of hamstrings	1 minutes	Static stretching of the hamstrings with sitting position. Both legs spread out. Knee was fully extended. Torso bent over the leg. Thirty seconds for each side.
Stretching of quadriceps	1 minutes	Static stretching of the quadriceps with laterally sitting position. Knee was fully flexed, and ankle was hold behind the buttocks. Hip was extended as much as possible. Thirty seconds for each side.

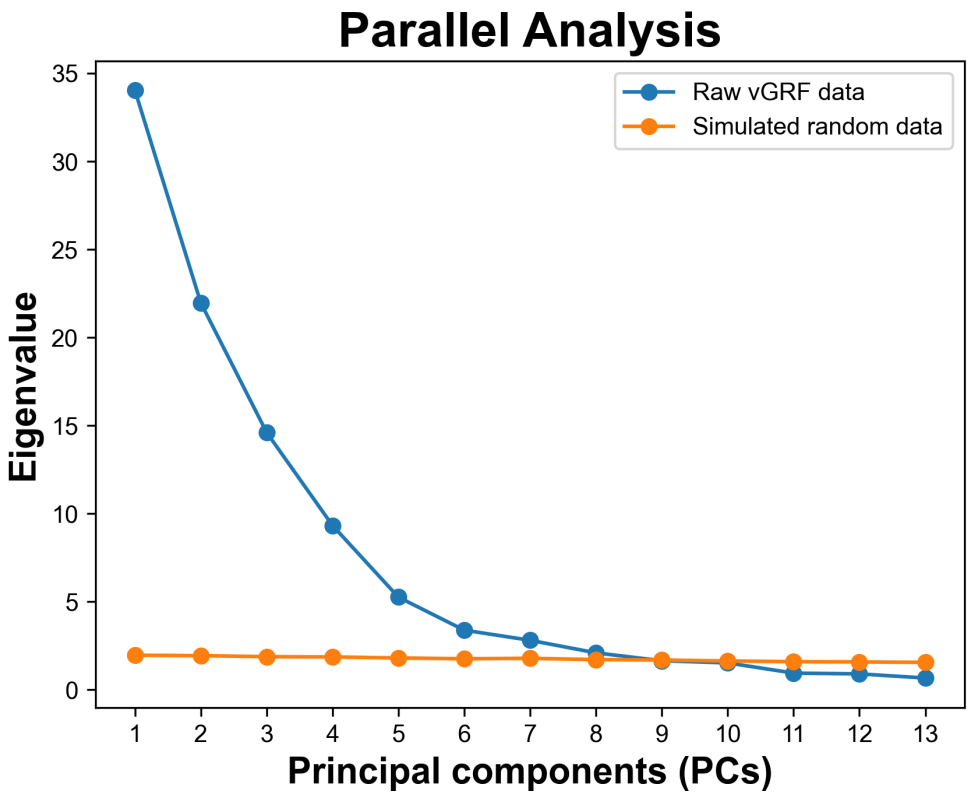

Figure S2. Scree plots with parallel analysis indicating the number of principal components to be selected. The blue line represents the trend of changes in eigenvalues during principal component analysis (PCA) using raw vertical ground reaction force (vGRF) data. The orange line represents the trend of changes in eigenvalues during PCA using the same vGRF dataset, but the temporal structure was randomly reordered.

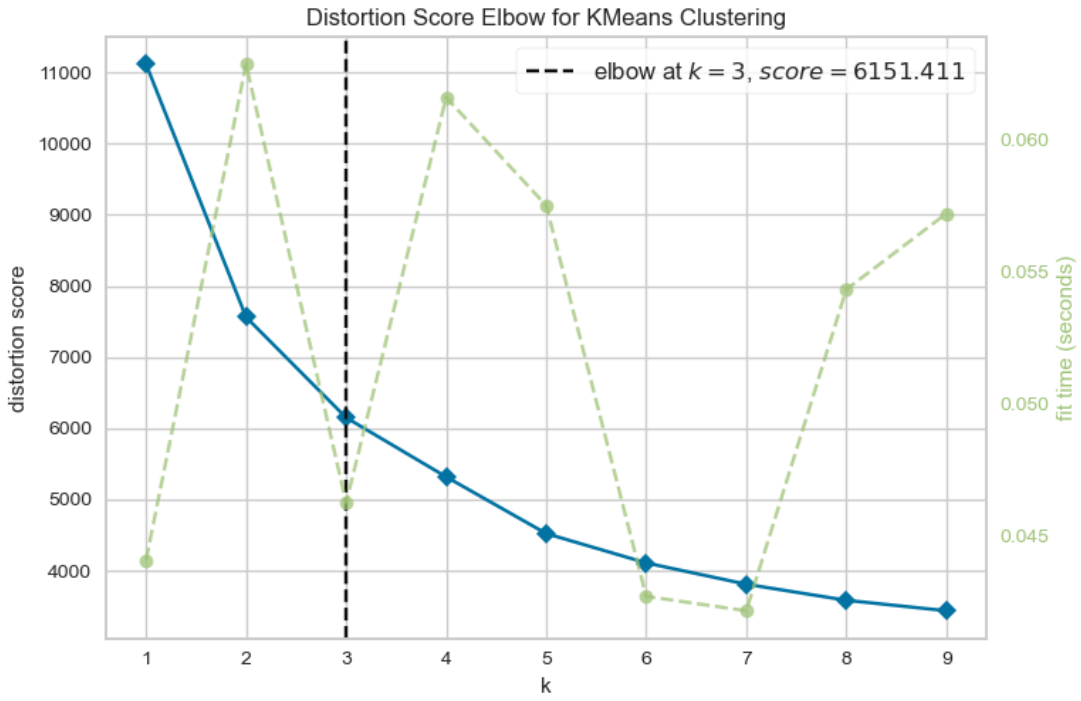

Figure S3. Result of elbow method to determine k value for clustering. The solid blue line showed that the distortion score decreases as the value of k increases. The green dashed line represents the time required to fit the k-means method. By combining these two parameters (small distortion score and short fit time), the optimal "elbow point" was ultimately selected at k=3 (indicated by the black dashed line).

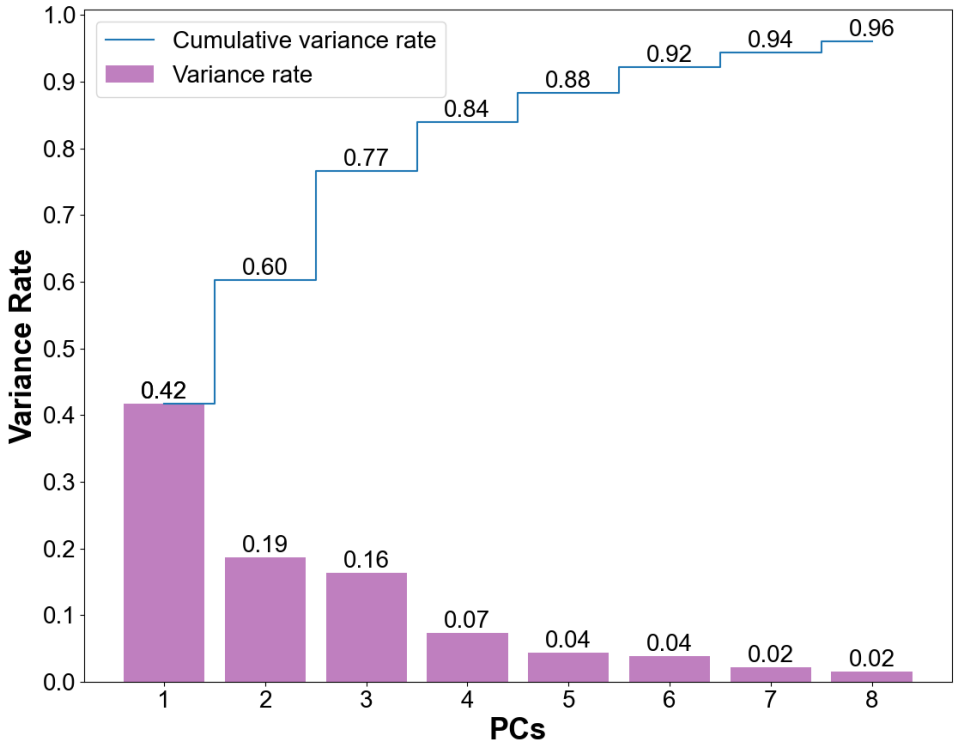

Figure S4. The variance rate and cumulative variance rate of the first 8 PCs. The horizontal axis represents the number of principal components (PCs). The vertical axis represents variance rate, which explains the percentage of the raw data set.